Importance of Steric Effects in Cluster Models of Silicon Surface Chemistry: ONIOM Studies of the Atomic Layer Deposition (ALD) of Al_2O_3 on H/Si(111)[†]

Mathew D. Halls and Krishnan Raghavachari*

Department of Chemistry, Indiana University, Bloomington, Indiana 47405-7102

Received: October 7, 2003; In Final Form: January 19, 2004

Cluster based density functional calculations have been carried out to examine the effect of steric interactions on chemical reactions at the H/Si(111) surface, adopting the initial Al_2O_3 atomic layer deposition (ALD) surface reactions involving H_2O and $Al(CH_3)_3$ (TMA) as our test reactions. Results obtained for the minimal $Si_{10}H_{16}$ cluster and two larger $Si_{43}H_{46}$ ONIOM embedded clusters reveal a substantial difference of up to 0.28 eV (6 kcal/mol) in the predicted activation energies involving TMA, revealing the inadequacy of small clusters to model atomically dense semiconductor surfaces.

I. Introduction

The computational investigation of surface-molecule interactions and the subsequent chemical reactions is a rapidly growing research area. Although slab calculations involving plane waves and periodic boundary conditions are employed widely in the physics community, cluster models with atom-centered Gaussian functions have been successfully used in the quantum chemistry community to investigate a variety of surface chemical phenomena, particularly in covalently bonded semiconductors such as silicon. A key question in such cluster calculations is the convergence of the calculated properties as a function of the size of the cluster.

As a cluster model increases in size, accurate treatment of the entire structure quickly becomes intractable. For such large systems a particularly cost-effective solution is the embedded cluster or hybrid method approach, in which the reaction site is represented by a molecular cluster of surface atoms that is immersed in a larger structure, and the two regions are treated with different levels of theory.[1] This technique reduces the overall computational cost while retaining the salient features of the true extended surface. The application of this approach to condensed phase systems, such as solids and surfaces, is increasing in activity. For example, Gordon and co-workers used a quantum mechanics/molecular mechanics (QM/MM) scheme to examine the adsorption of H_2O[2] and the oxidation by atomic O[3] of bare Si(100) surfaces. In this paper, we use embedded cluster models to demonstrate the importance of steric effects in the description of reactive chemistry using cluster models.

Current efforts in several research groups are directed toward the investigation of Al_2O_3 growth via atomic layer deposition (ALD) as a replacement dielectric for SiO_2 for use in microelectronics applications. Al_2O_3 growth by ALD involves film deposition through the cycling of self-terminating surface reactions, providing highly uniform conformal films with thickness control at the atomic layer level.[4] Each half-reaction involves exposure of the substrate to a gas-phase precursor, resulting in a maximum growth rate of one monolayer per exposure. The most often used precursors for Al_2O_3 growth are trimethylaluminum ($Al(CH_3)_3$, TMA) and H_2O, as the aluminum and oxygen precursors, respectively. The Al_2O_3 ALD growth mechanism has been the focus of both experimental and theoretical studies.[5,6] Upon exposure of the substrate, TMA reacts readily with surface O−H groups, depositing $-Al(CH_3)_2$ on the surface and liberating CH_4. Subsequent treatment of the Al surface species with H_2O results in new surface O−H groups, again releasing CH_4. In our group, recent efforts have been directed toward examining the energetics and atomistic details of chemical reaction paths for Al_2O_3 growth on technologically relevant substrates. Previously, we have studied the initial surface reaction pathways for TMA, H_2O, and the precursor side-reaction product dimethylaluminum hydroxide ($Al(CH_3)_2$-OH, DMAOH) interacting with the 2×1 reconstructed hydrogen-terminated Si(100) surface.[7,8] In that work, the dominant surface reactions were found to be those with direct implication in the Al_2O_3 ALD growth mechanism, leading to the formation of Si−Al and Si−O surface linkages. Due to the difference in the size of the H_2O and TMA reactants and the newly understood mechanistic details, the critical Al_2O_3 ALD surface reactions are well-suited as model reactions to examine the size dependence of cluster surface models.

Despite the central role the Si(100)-2×1 surface plays in semiconductor devices, surface roughness and a high density of chemical defect sites can dramatically complicate the interpretation of experimental data obtained in studies of chemistry at Si surfaces. The Si(111) surface is the most thermodynamically stable face of Si and can form near-perfect atomically flat, ideally hydrogen-passivated terraces.[9] As such, it is often studied to gain understanding into the more complex chemical behavior of the atomically rough Si(100)-2×1 surface.[10] However, the Si(111) surface is known to be less reactive than the Si(100) surface. Etching experiments on Si(111) highlight the important influence steric hindrance plays in determining the local reactivity of surface sites.[11,12] Structurally, the Si(111) surface is much more atomically dense than the 2×1 reconstructed Si(100) surface, which is characterized by the row−trench corrugation. The Si(111) surface silicon interatomic distance is only ca. 3.8 Å, which may give rise to increased barrier heights and less favorable reaction enthalpies due to surface steric interactions.

Work by Widjaja and Musgrave has shown, for investigations into bare Si(100), the reasonably small $Si_{21}H_{20}$ three-dimer

[†] Part of the special issue “Fritz Schaefer Festschrift”.

* Corresponding author. E-mail: kraghava@indiana.edu.

10.1021/jp037014m CCC: $27.50 © 2004 American Chemical Society
Published on Web 03/03/2004

cluster model is sufficient to represent the surface reaction site, with the major steric interactions stemming from neighboring dimers within a dimer row.[13] Moreover, most of the theoretical studies of silicon surface chemistry to date have successfully employed a minimal Si_9H_{12} cluster that has been shown to accurately reproduce the local chemistry of the Si(100)-2×1 surface.[7,8,14−18] Atomically dense semiconductor surfaces, such as H/Si(111), may require larger cluster models to obtain reaction energetics representative of the real surface.

In the present work, first-principles calculations based on hybrid density functional theory are carried out on silicon clusters and embedded cluster models to investigate the reaction enthalpies and atomistic details for the initial Al_2O_3 ALD surface reactions on H/Si(111). The multilayer ONIOM method of Morokuma and co-workers[19] is used to effectively provide a realistic steric environment for reactions at H/Si(111) and, through comparison to results from a minimal surface cluster model, provide valuable insight into the influence of steric interactions on the chemical reactivity of the H/Si(111).

II. Computational Details and Surface Models

The calculations presented in this work were carried out using the Gaussian 03 suite of electronic structure programs.[20] All results described here are obtained using the B3-LYP hybrid functional, which corresponds to Becke's three-parameter exchange functional (B3) along with the Lee−Yang−Parr gradient-corrected correlation functional (LYP).[21,22] The simplest cluster model used here is exactly analogous to the Si_9H_{14} model used in our previous studies of Al_2O_3 ALD reactions on the Si(100)-2×1 surface.[7,8] Shown in Figure 1 (top), this cluster corresponds roughly to one unit cell of the H/Si(111) surface, consisting of 10 silicon atoms. This cluster closely reproduces the local structure around the single surface reaction site and consists of the Si atom of the surface reaction site, three second-layer Si atoms, three third-layer Si atoms, and three fourth-layer Si atoms. The cluster is terminated by hydrogen atoms to satisfy the valency of the cleaved Si−Si bonds during excision from the extended surface, giving a cluster stoichiometry of $Si_{10}H_{16}$ (analogous to adamantane, $C_{10}H_{16}$). Boundary constraints, fixing atoms to their bulk tetrahedral positions, are imposed on the third- and fourth-layer silicons to avoid unphysical structural relaxation. The terminal hydrogens that represent third- or fourth-layer silicons are held fixed at positions corresponding to a Si−H distance of 1.48 Å along ideal tetrahedral directions. A multilevel basis set is employed in this work, denoted here as dzdp, representing the first- and second-layer cluster atoms as well as the TMA and H_2O atoms with the 6-31G** basis set and the lower layer frozen cluster atoms with the 6-31G basis set.[23,24]

For comparison, two larger embedded cluster models consisting of roughly seven surface unit cells, corresponding to the minimal Si_{10} cluster surrounded by six nearest neighbor Si_{10} clusters are also used. They are represented using the hybrid cluster embedding scheme of Morokuma (ONIOM)[19] in which the total energy of a two-region system is defined as

$$E(\text{region } 1+2) = E_{\text{low}}(\text{region } 1+2) - E_{\text{low}}(\text{region } 1) + E_{\text{high}}(\text{region } 1)$$

where region 1 is the cluster containing the reaction site, treated with a high level of theory and region 2 is the surrounding region treated less accurately. Here, the higher and lower levels of theory are differentiated only by the basis set employed, namely, 6-31G** and STO-3G.[25] The composite ONIOM H/Si(111) surface models have a stoichiometry of $Si_{43}H_{46}$ and differ only in the atoms included in the high and low regions. The chemical termination and structural constraints imposed are identical to those applied to the $Si_{10}H_{16}$ cluster. Figure 1 illustrates the two ONIOM models used in this work, denoted Si_{43}-**I** and Si_{43}-**II** (middle and bottom), with the high and low regions rendered as balls and sticks and as tubes, respectively. As shown there, in the Si_{43}-**I** model, the central Si_{10} cluster is represented with the 6-31G** basis set and the surrounding atoms are represented using the STO-3G basis, whereas in the Si_{43}-**II** model, the first- and second-layer silicons along with the surface hydrogens are represented with the 6-31G** basis and then lower-layer atoms are represented using STO-3G. As above, in calculations involving the ONIOM H/Si(111) surface models, the TMA and H_2O atoms are also represented with the 6-31G** basis set.

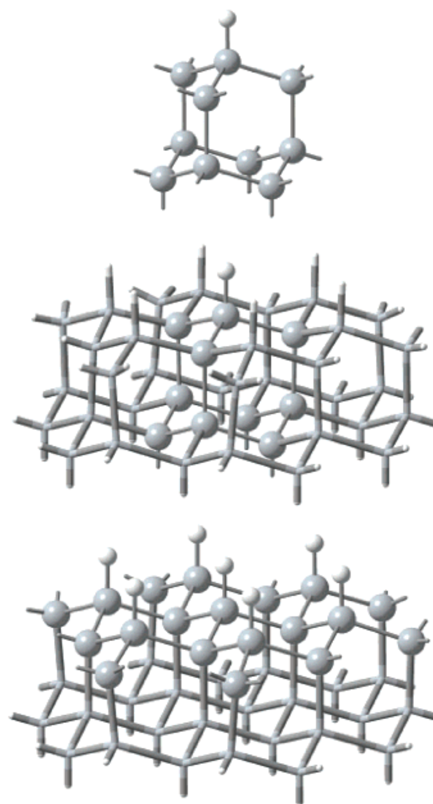

Figure 1. Structures of the $Si_{10}H_{16}$ (top) and $Si_{43}H_{46}$ embedded cluster models used to represent the reaction site on the H/Si(111) surface in this work. For the embedded cluster models, atoms rendered as ball-and-stick and tubes are represented using the 6-31G** and STO-3G basis sets, respectively, giving rise to the ONIOM Si_{43}-**I** (middle) and ONIOM Si_{43}-**II** (bottom) surface models. (Terminal hydrogens omitted for clarity.)

Subject to the Si cluster boundary constraints, minimum energy structures were calculated for the reactants, transition structures, and product species for initial surface reactions of TMA and H_2O with the H/Si(111) reaction site models. The nature of the calculated structures was verified by subsequent harmonic frequency calculations, which also yielded zero-point energy (ZPE) corrections. All enthalpies reported here include ZPE corrections. To obtain an estimate of the basis set converged enthalpies, single-point energy calculations were performed on the optimized structures for the $Si_{10}H_{16}$ cluster using the 6-311G(2df,2p) basis set,[26] and on the Si_{43}−**II** structures representing the first- and second-layer atoms and the TMA and H_2O atoms with the 6-311G(2df,2p) basis set, and the lower-layer atoms with the 6-31G basis.

TABLE 1: Representative Bond Lengths and Relative Enthalpies of Critical Structures for Reactions of H_2O with Cluster and Embedded Cluster Models of the H/Si(111) Surface Calculated at the B3-LYP/dzdp and B3-LYP/(6-31G:STO-3G) Levels of Theory**

	bond lengths[a] (Å)			rel energy[b] (eV)		
	Si−O	Si−H	O−H	$Si_{10}H_{16}$	$Si_{43}H_{46}$ (I)	$Si_{43}H_{46}$ (II)
H_2O and H/Si reactants		1.49	0.97	0.00	0.00	0.00
Si−H···H_2O complex[‡]	3.88	1.49	0.97	−0.11	−0.08	−0.08
[Si−H + H_2O → Si−OH + H_2]	1.93	1.81	1.15	1.64	1.64	1.59
Si−OH and H_2 products	1.69			−0.68	−0.69	−0.72

[a] Bond lengths are for structures calculated with the ONIOM embedded cluster Si_{43}-**II**. [b] ZPE corrected relative enthalpy calculated with respect to separated reactant species.

III. Results and Discussion

A. Reactant Surface Complexes. The $Si_{10}H_{16}$ cluster used to represent the reaction site is shown in Figure 1 (top), representing one unit cell of the H/Si(111) surface, analogous to the Si_9H_{14} cluster commonly used to study chemical reactions at the H/Si(100)-2×1 surface. As H_2O approaches the Si_{10} cluster, it forms a weakly bound reactant-like surface complex that is calculated to be 0.11 eV lower in energy than the separated reactants. TMA [$Al(CH_3)_3$] is also found to form a reactant complex with the single surface unit cluster that is bound by only 0.04 eV. The two $Si_{43}H_{46}$ ONIOM embedded cluster models are also shown in Figure 1. The Si_{43}-**I** model (middle) assigns the larger basis set to the central Si_{10} reaction site with a minimal basis representing all the surrounding atoms. The Si_{43}-**II** model (bottom) assigns the larger basis to the upper surface slab composed of the surface hydrogens, the first- and second-layer silicons, with a minimal basis set for the lower atoms. Calculations using the Si_{43} embedded cluster models both give a surface H_2O binding energy of 0.08 eV. TMA is only slightly bound with an adsorption energy of −0.04 and −0.01 eV, respectively, for the Si_{43}-**I** and Si_{43}-**II** H/Si(111) surface models. The H/Si(111)−H_2O and −TMA surface binding energies, summarized in Tables 1 and 2, are comparable to the surface adsorption energies previously computed for H/Si(100)-2×1 (0.16 and 0.03 eV, for H_2O and TMA, respectively).[7]

B. Reaction between H_2O and H/Si(111). First we will examine the major reaction pathway involving the smaller reactant, H_2O. Following exposure of the H/Si surface to H_2O, two potential reaction pathways may occur: proton exchange in which a proton is simultaneously abstracted and deposited at the surface reaction site or surface hydroxylation in which −OH is deposited on the surface and H_2 is released. In our previous work, we examined the relative energetics for these pathways occurring at the H/Si(100)-2×1 surface and found that the activation energy for the H-exchange pathway is ca. 0.7 eV higher in energy than that of the competing hydroxylation pathway.[7] Given the central role surface −OH groups play in the ALD growth mechanism of Al_2O_3,[5,6] we will restrict our discussion here to the dominant H/Si(111) surface hydroxylation pathway:

$$\text{Si−H}^* + H_2O \rightarrow \text{Si−OH}^* + H_2 \qquad \text{(a)}$$

where the surface species is denoted by asterisks.

The relative reaction enthalpies for the surface hydroxylation pathway (reaction a) are listed in Table 1, along with representative bond lengths for the critical point structures. As shown there, the activation energy and overall enthalpy using the $Si_{10}H_{16}$ cluster are determined to be +1.64 and −0.68 eV, respectively, which is only 0.06 and 0.01 eV larger than the Si_9H_{14} results obtained for the H/Si(100)-2×1 surface.[7] Using the embedded cluster models, Si_{43}-**I** and -**II**, the hydroxylation pathway is similarly favorable, being exothermic by −0.69 and −0.72 eV. The barrier heights using the larger clusters also agree well with that obtained with the Si_{10} cluster, having values of 1.64 and 1.59 eV (for Si_{43}-**I** and Si_{43}-**II**). The transition state structure is shown in Figure 2a. As expected, the hydroxylation pathway transition state has Si−H and O−H bonds elongated by 0.31 and 0.19 Å compared to the surface complex structural parameters, consistent with the ultimate breaking of these bonds. The Si−O distance decreases throughout the reaction from 3.88 Å in the H_2O−surface complex, becoming 1.93 Å in the activated complex ,and the final surface product structure has a Si−O bond length of 1.69 Å. Comparison of the reaction energies in Table 1 shows that the activation energies and reaction exothermicities calculated using the minimal H/Si(111) surface reaction site cluster are reasonably well conserved when compared to energies computed using the much larger ONIOM surface models, $Si_{43}H_{46}$-**I** and -**II** (less than 0.05 eV difference). The close agreement in not surprising considering the small size of the H_2O molecule. Results obtained using the larger basis set predict a barrier height and reaction enthalpy of +1.67 and −0.73 eV for the Si_{10} cluster, and +1.62 and −0.80 eV for the Si_{43}-**II** embedded cluster. The reaction energy profiles for the H/Si(111) hydroxylation reaction calculated for the Si_{10} and Si_{43}-**II** models are shown in Figure 3a (critical structures denoted by ● and ○, respectively) illustrating the close agreement between the small and large surface cluster results.

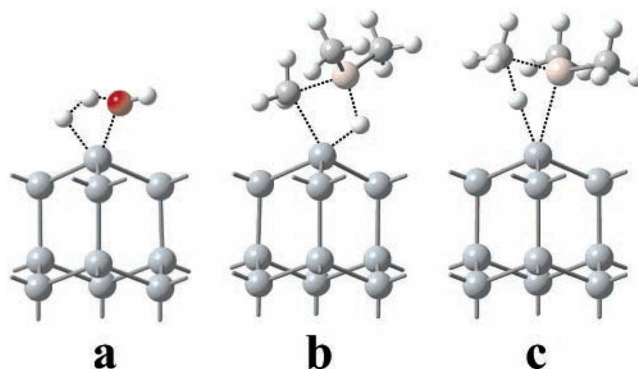

Figure 2. B3-LYP/dzdp optimized transition structures for (a) the surface hydroxylation reaction between H_2O and H/Si(111), (b) the CH_3/H exchange reaction, and (c) the CH_3 release reaction between TMA [$Al(CH_3)_3$] and the H/Si(111) surface.

In an earlier study, Tada and Yoshimura[27] used ab initio methods to investigate the hydroxylation of H/Si(111) using a simple H−Si(SiH_3)$_3$ cluster as a surface model. Using the MP4//HF/6-31G* level of theory, H/Si(111) surface hydroxylation was determined to be 0.7 eV exothermic, which is comparable to the results presented here.

C. Reactions between TMA and H/Si(111). Next, we will consider the competing surface reactions for TMA. TMA is a significantly larger reactant than H_2O; therefore one might expect a difference in the relative sensitivity to cluster size used

TABLE 2: Representative Bond Lengths and Relative Enthalpies of Critical Structures for Reactions of TMA ($Al(CH_3)_3$) with Cluster and Embedded Cluster Models of the H/Si(111) Surface Calculated at the B3-LYP/dzdp and B3-LYP/(6-31G:STO-3G) Levels of Theory**

	bond lengths[a] (Å)				rel energy[b] (eV)		
	Si−Al	Si−H	Al−C	Si−C	$Si_{10}H_{16}$	$Si_{43}H_{46}$ (I)	$Si_{43}H_{46}$ (II)
TMA and H/Si reactants		1.49	1.97	-	0.00	0.00	0.00
Si−H···TMA complex	4.15	1.50	1.98	4.68	−0.04	−0.04	−0.01
$[Si-H + TMA \rightarrow Si-CH_3 + HAl(CH_3)_2]^{\ddagger}$		1.70	2.11	2.40	1.50	1.63	1.69
$[Si-H + TMA \rightarrow Si-Al(CH_3)_2 + CH_4]^{\ddagger}$	2.86	1.89	2.13		1.23	1.45	1.49
$Si-CH_3$ and $H-Al(CH_3)_2$ products				1.91	0.09	0.14	0.10
$Si-Al(CH_3)_2$ and CH_4 products	2.50				−0.38	−0.28	−0.33

[a] Bond lengths are for structures calculated with the ONIOM embedded cluster Si_{43}-**II**. [b] ZPE corrected relative enthalpy calculated with respect to separated reactant species.

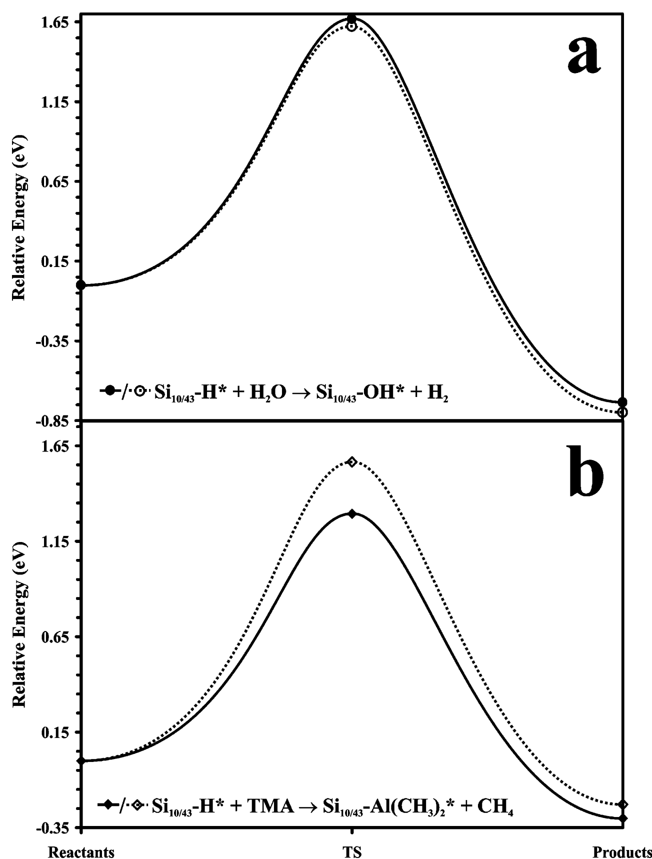

Figure 3. Reaction energy profiles for the initial surface reaction pathways between (a) H_2O and (b) TMA [$Al(CH_3)_3$] with the H/Si(111) surface. Energies calculated at the B3-LYP/6-311G(2df,2p) level of theory using the critical points for the $Si_{10}H_{16}$ cluster and the $Si_{43}H_{46}$ (Si_{43}-**II**) ONIOM cluster as described in the text.

in investigating H/Si(111) surface reaction pathways. For TMA reacting with the H/Si(111) surface there are two low-energy surface reaction pathways:[7]

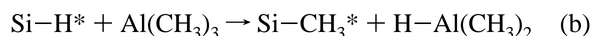

$$Si-H^* + Al(CH_3)_3 \rightarrow Si-CH_3^* + H-Al(CH_3)_2 \quad (b)$$

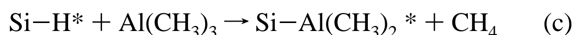

$$Si-H^* + Al(CH_3)_3 \rightarrow Si-Al(CH_3)_2{}^* + CH_4 \quad (c)$$

where the surface species are denoted by asterisks. Reaction pathway b is the CH_3/H exchange pathway in which TMA approaches the H/Si(111) surface and simultaneously transfers a methyl group to and abstracts a hydrogen from the surface reaction site. The reaction energies and characteristic critical point bond lengths for this reaction pathway are presented in Table 2. Calculations using the Si_{10} cluster predict a classical barrier height of 1.5 eV for this reaction, which is ca. 0.09 eV larger than that for the H/Si(100).[7] The transition structure for the CH_3/H exchange pathway is shown in Figure 2b. During the reaction, the Si−C bond changes from 4.68 Å in the TMA−surface complex, to 2.40 Å at the transition state, finally becoming 1.91 Å in the $Si-CH_3$* product. The activation energy for this reaction pathway calculated with the Si_{43}-**I** and Si_{43}-**II** clusters is 1.63 and 1.69 eV, respectively, which are 0.13 and 0.19 eV larger than that for the smaller cluster, indicating significant steric interactions between TMA and the H/Si(111) surface, which are absent in the single surface reaction site model. For the overall reaction enthalpy, the calculations agree reasonably well, having an endothermicity of 0.09, 0.14, and 0.10 eV for the Si_{10}, Si_{43}-**I**, and Si_{43}-**II** clusters, respectively. Activation energies using the large basis for the Si_{10} and Si_{43}-**II** clusters are 1.52 and 1.73 eV, respectively.

In reaction c, TMA reacts with H/Si(111), resulting in the loss of CH_4 and deposition of $-Al(CH_3)_2$ surface species. Together with reaction a, the surface hydroxylation pathway, reaction c is of primary interest in this work because they result in the formation of Si−O and Si−Al linkages on the H/Si(111) surface, which are clearly implicated in the ALD growth of Al_2O_3. The characteristic bond lengths and relative enthalpies for $-Al(CH_3)_2$ deposition are presented in Table 2 and the transition structure is shown in Figure 2c. The Si−Al distance decreases over the course of the reaction from a value of 4.15 Å in the surface complex, becoming 2.86 Å in the transition state and the final product has a Si−Al bond length of 2.50 Å. Conversely, the Al−C distance increases, being elongated at the transition structure by 0.15 Å. The energy of the activated complex for the CH_4 release pathway is computed to be 1.23 eV with the Si_{10} cluster. As with the CH_3/H exchange pathway, the activation energy computed using the single H/Si(111) unit cluster significantly underestimates the reaction barrier compared to energies for the ONIOM embedded clusters. The barrier heights computed using the Si_{43}-**I** and Si_{43}-**II** models are 0.22 and 0.26 eV larger than that with the Si_{10} cluster, clearly demonstrating significant cluster size dependence. The CH_4 release pathway is predicted to have an overall enthalpy of −0.38, −0.28, and −0.33 eV, using the Si_{10}, Si_{43}-**I**, and Si_{43}-**II** models considered here. Larger basis set calculations comparing the Si_{10} and Si_{43}-**II** critical points structure energies indicate that the smaller cluster underestimates the activation energy by 0.28 eV and overestimates the exothermicity by 0.07 eV, compared to a barrier height and exothermicity of 1.57 and 0.23 eV. Once again, the reaction energy profiles for the small and larger H/Si(111) cluster models for the $-Al(CH_3)_2$ deposition pathway are shown in Figure 3b (denoted ◆ and ◇, respectively).

The results described here for the $-Al(CH_3)_2$ deposition pathway (reaction c) can be compared to a theoretical study by Matsuwaki, Nakajima, and Yamashita.[28] Reactions between

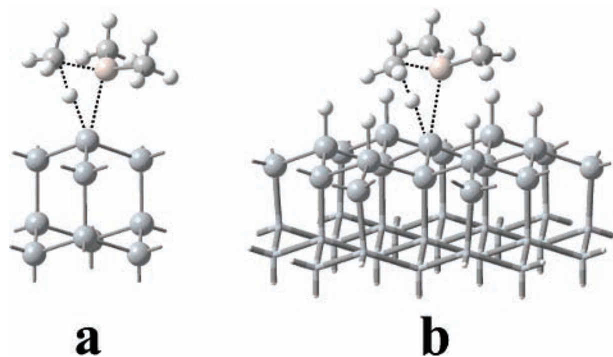

Figure 4. Optimized $-Al(CH_3)_2$ deposition pathway transition structures for the single surface unit $Si_{10}H_{16}$ cluster and the $Si_{43}H_{46}$ (Si_{43}-**II**) ONIOM embedded cluster illustrating the small H/Si(111) surface hydrogen−TMA distances in the Si_{43}-**II** model. (Terminal hydrogens omitted for clarity.)

dimethylaluminum ($HAl(CH_3)_2$, DMAH) and a model H/Si(111) surface were investigated using gradient-corrected density functional theory and a double-ζ basis set. Representing the H/Si(111) surface by a single layer of hydrogen terminated silicons, they found a barrier height and reaction exothermicity of 1.45 and 0.30 eV for the reaction analogous to reaction c between DMAH and H/Si(111), which are in reasonable agreement to the ONIOM B3-LYP/(6-31G**:STO-3G) enthalpies reported here.

The origin of the increase in the barrier for TMA on going to the larger cluster is clearly due to repulsive steric interactions involving the larger molecule. Figure 4 shows the $-Al(CH_3)_2$ deposition transition state structures involving TMA for the small $Si_{10}H_{16}$ cluster model and the larger ONIOM Si_{43}-**II** model (parts a and b, respectively). For the small cluster the TMA approaches the surface in a flat orientation. If the same orientation is then embedded in a larger cluster (not shown), it would result in nonbonded distances between the hydrogens of the passive methyl groups and the neighboring H/Si(111) surface hydrogens as close as 1.4−1.5 Å. This is clearly unfavorable because such distances are considerably shorter than the sum of the van der Waals radii for the two hydrogens (2.4 Å). This causes a slight tilt as well as rotation of the methyl groups in the transition state for the larger Si_{43}-**II** model (Figure 4b), resulting in the closest nonbonded H−H distance having a more reasonable value of 2.27 Å. Other distances such as Si−Al (2.73 Å in Figure 4a vs 2.86 Å in Figure 4b) and Si−C (3.42, 3.78, and 3.80 Å in Figure 4a vs 3.46, 4.01, and 4.03 Å in Figure 4b) also reflect the same effect.

As the size of the molecular cluster used to model the silicon (111) surface increases, the number of subsurface silicon atoms (second- and third-layer atoms) also increase proportional to the first- and second-layer silicon atoms. In addition to defining the surface reaction site where the bond breaking and formation occurs, the topmost atomic layers also give rise to the majority of the steric interactions discussed here. The effect of the lower layers is largely structural, providing physically realistic geometric restrictions to the surface model. In the Si_{43}-**II** model, the boundary between the constrained and unconstrained layers also separates the regions represented by a low and high level of theory. A comparison of the energies for the critical points for only the high-level region with the total energies for the composite Si_{43}-**II** model provides an estimate of the steric effects contributed by the lower Si layers. We find that the steric contributions from the lower-layer atoms are very small, with the energies agreeing to within 0.04 eV. To evaluate the effect of the geometric constraints provided by the lower Si layers on the reaction enthalpies, additional calculations were carried out for a subset of the Si_{43}-**II** embedded cluster model. The activation energies and overall enthalpies for the TMA−surface reactions were calculated at the B3-LYP/6-31G** level of theory for a fully relaxed hydrogen-terminated Si cluster with stoichiometry $Si_{19}H_{34}$, which corresponds to the topmost layers in the Si_{43}-**II** embedded cluster without the constraining lower layers. Comparison of the relaxed structure results with those obtained with the full Si_{43}-**II** model indicates that the geometric constraints have a minor effect on the reaction energetics for growth processes occurring on the topmost Si layer. The differences in barrier heights for the H/CH_3 and the Si−Al linkage formation pathways are only 0.11 and 0.10 eV, respectively. Despite the small energetic differences between the constrained and fully relaxed models, the structural changes are dramatic. Structurally, the minimum energy configuration for the fully relaxed $Si_{19}H_{34}$ cluster is no longer a faithful representation of the Si(111) surface, being distorted considerably.

In summary, the results presented here highlight the crucial role steric interactions play in determining the chemical reactivity at H/Si(111) surfaces, with implications for the application of cluster-based quantum chemical methods to atomically dense surfaces, in general. Comparison of the activation energies and reaction enthalpies for surface reaction pathways between the smaller H_2O and larger TMA reactants, obtained using the minimal $Si_{10}H_{16}$ cluster and the larger $Si_{43}H_{46}$ embedded clusters, clearly illustrates the effect of steric hindrance in increasing the activation energies thereby reducing the chemical reactivity of the H/Si(111) surface. For the surface reaction pathway involving H_2O, the energetics are largely insensitive to cluster size, with all three H/Si(111) surface models furnishing similar results to within ∼0.05 eV (1 kcal/mol). The activation energies for the TMA surface reactions using the $Si_{43}H_{46}$ embedded cluster models are ∼0.25 eV larger (6 kcal/mol) than the $Si_{10}H_{16}$ energies, which is symptomatic of significant shortcomings in the use of minimal cluster models to investigate chemistry at the H/Si(111) surface.

IV. Conclusions

The role of steric hindrance in determining the relative chemical reactivity of the H/Si(111) surface has been investigated by examining the initial surface reactions between the Al_2O_3 ALD precursors, TMA and H_2O, and the H/Si(111) surface using density functional cluster and ONIOM embedded cluster calculations. Significant differences are noted in the cluster size dependence of the reaction barriers between the smaller and larger reactants, H_2O and TMA. The energetics for the surface hydroxylation reaction between H_2O and the $Si_{10}H_{16}$ and $Si_{43}H_{16}$ cluster models of the H/Si(111) surface are in close agreement to within 0.05 eV (1 kcal/mol). However, activation energies for the TMA pathways differ by up to 0.28 eV (6 kcal/mol) between the minimal $Si_{10}H_{16}$ cluster and the more extensive $Si_{43}H_{46}$ embedded cluster models, due to steric hindrance from the larger molecule interacting with the surface. This work clearly demonstrates the importance of employing cluster models of sufficient size when investigating chemical processes at atomically dense surfaces

Acknowledgment. We gratefully acknowledge computational resources provided by the University Information Technology Services (UITS), Indiana University, and a grant from NCSA (Grant No. CHE030049). M.D.H. also thanks the Department of Chemistry, Indiana University, for financial

support provided by an Ernest R. Davidson postdoctoral fellowship. Helpful discussions with M.M. Frank and Y. J. Chabal are also acknowledged.

References and Notes

(1) Froese, R. D. J.; Morokuma, K. In *Encyclopedia of Computational Chemistry*; Schleyer, P. v. R., Ed.; John Wiley & Sons: Ltd.; New York, 2003.

(2) Jung, Y. S.; Choi, C. H.; Gordon, M. S. *J. Phys. Chem. B* **2001**, *105*, 4039.

(3) Choi, C. H.; Liu, D. J.; Evans, J. W.; Gordon, M. S. *J. Am. Chem. Soc.* **2002**, *124*, 8730.

(4) George, S. M.; Ott, A. W.; Klaus, J. W. *J. Phys. Chem.* **1996**, *100*, 13121.

(5) Yates, D. J. C., Dembinski, G. W.; Kroll, W. R.; Elliott, J. J. *J. Phys. Chem.* **1969**, *73*, 911.

(6) Widjaja, Y.; Musgrave, C. B. *Appl. Phys. Lett.* **2002**, *80*, 3304.

(7) Halls, M. D.; Raghavachari, K. *J. Chem. Phys.* **2003**, *118*, 10221.

(8) Halls, M. D.; Raghavachari, K.; Frank, M. M.; Chabal, Y. J. *Phys. Rev. B* **2003**, *68*, 161302R.

(9) Chabal, Y. J.; Higashi, G. S.; Raghavachari, K.; Burrows, V. A. *J. Vac. Sci. Technol. A* **1989**, *7*, 2104.

(10) Frank, M. M.; Chabal, Y. J.; Wilk, G. D. *Appl. Phys. Lett.* **2003**, *82*, 4758.

(11) Jakob, P.; Chabal, Y. J.; Raghavachari, K.; Becker, R. S. *Surf. Sci.* **1992**, *275*, 407.

(12) Flidr, J.; Huang, Y.-C.; Newton, T. A.; Hines, M. A. *J. Chem. Phys.* **1998**, *108*, 5542.

(13) Widjaja, Y.; Musgrave, C. B. *Surf. Sci.* **2000**, *469*, 9.

(14) Weldon, M. K.; Stefanov, B. B.; Raghavachari, K.; Chabal, Y. J. *Phys. Rev. Lett.* **1997**, *79*, 2851.

(15) Raghavachari, K.; Chabal, Y. J.; Struck, L. M. *Chem. Phys. Lett.* **1996**, *252*, 230.

(16) Konecny, R.; Doren, D. J. *J. Chem. Phys.* **1997**, *106*, 2426.

(17) Stefanov, B. B.; Raghavachari, K. *Appl. Phys. Lett.* **1998**, *73*, 824.

(18) Stefanov, B. B.; Gurevich, A. B.; Weldon, M. K.; Raghavachari, K.; Chabal, Y. J. *Phys. Rev. Lett.* **1998**, *81*, 3908.

(19) Svensson, M.; Humbel, S.; Froese, R. D. J.; Matsubara, T.; Sieber, S.; Morokuma, K. *J. Phys. Chem.* **1996**, *100*, 19357.

(20) Frisch, M. J.; et al. *Gaussian 03*, Revision A.1; Gaussian, Inc.: Pittsburgh, PA, 2003.

(21) Becke, A. D. *J. Chem. Phys.* **1993**, *98*, 5648.

(22) Lee, C.; Yang, W.; Parr, R. G. *Phys. Rev. B* **1988**, *37*, 785.

(23) Hariharan, P. C., Pople, J. A. *Theor. Chim. Acta* **1973**, *28*, 213.

(24) Francl, M. M.; Petro, W. J.; Hehre, W. J.; Binkley, J. S.; Gordon, M. S.; DeFrees, D. J.; Pople, J. A. *J. Chem. Phys.* **1982**, *77*, 3654.

(25) Hehre, W. J.; Stewart, R. F.; Pople, J. A. *J. Chem. Phys.* **1969**, *51*, 2657.

(26) Krishnan, R.; Binkley, J. S.; Seeger, R.; Pople, J. A. *J. Chem. Phys.* **1980**, *72*, 650.

(27) Tada, T.; Yoshimura, R. *Phys. Lett. A* **1996**, *220*, 224.

(28) Matsuwaki, T.; Nakajimia, T.; Yamashita, K. *J. Phys. IV Fr.* **2001**, *11*, 63.